Static, fatigue and impact behaviour of an autoclaved Flax Fibre Reinforced Composite for aerospace engineering

Tulio Halak Panzera[a, c], Thomas Jeannin[b], Xavier Gabrion[b], Vincent Placet[b], Chrystel Remillat[a], Ian Farrow[a], Fabrizio Scarpa[a]

[a]Bristol Composites Institute (ACCIS), University of Bristol, BS8 1 TR Bristol, UK

[b]Université Bourgogne Franche-Comté, FEMTO-ST Institute, CNRS/UFC/ENSMM/UTBM, Department of Applied Mechanics, 25000 Besançon, France

[c]Centre for Innovation and Technology in Composite Materials – CITeC, Department of Mechanical Engineering, Federal University of São João del Rei-UFSJ, Brazil.

Abstract. *This work describes the physical and mechanical characterisation of unidirectional* $[0]_{12}$ *and* crossply $[(0/90)_3/\bar{0}]_S$ flax *fibre reinforced composites fabricated in autoclave using a prepreg flax tape impregnated with fire retardant epoxy polymer. Tensile, bending and impact properties are evaluated along the longitudinal and transverse fibre directions. The tensile-tensile fatigue behaviour is characterised along the fibre direction. Physical and specific properties are also assessed to identify the potential characteristics of these bio-based composites for lightweight and secondary loadbearing applications. The robust manufacturing process described in this work, coupled with precision laser cutting, makes this type of composite a promising sustainable material for aircraft, transport and lightweight construction designs.*

Keywords: flax, epoxy, fire-retardant, quasi-static, fatigue, impact

1. Introduction

Flax, also known as common flax or linseed, is a member of the genus *Linum* in the family *Linaceae*. It is a food and fibre crop cultivated in cooler regions of the world [1]. Flax fibre is extracted from the bast beneath the surface of the stem of the flax plant. Within eight weeks of sowing, the plant can reach 100–150 mm in height and grows several centimetres per day under its optimal growth conditions, reaching 700–800 mm within 50 days [2]. At the microscopic scale, each elementary fibre is itself made of concentric cell walls, which differ from each other in terms of thickness and arrangement of their constitutive components. At the centre of the elementary fibre, the concentric cylinders with a small open channel in the middle called the lumen, which contributes to water uptake. The outer cell wall designed as the primary cell wall is only 0.2μm thick. On the outer side, the thin primary cell wall coats the thicker secondary cell wall which is responsible for the strength of the fibre and encloses the lumen. Each layer is composed of microfibrils of cellulose which run parallel one to another and form a micro fibrillar angle with the fibre direction; this angle is minimum in the secondary cell wall. This thickest cell wall contains numerous crystalline cellulose micro-fibrils and amorphous hemicellulose which are oriented at 10° with the fibre axis and give fibre its high tensile stiffness and strength [2, 3].

There is a significant amount of work in the open literature regarding the use of plant fibres, and in particular flax as reinforcement of composite materials [4]. Most of them are in the preliminary research and manufacturing stage and still require research efforts to address semi-structural and multifunctional applications. Among this abundant literature, only a few works focus on structural applications. Regarding flax, as recently reported by Blanchard and Sobey [5], only a few studies out of the hundreds published in recent years study the structural scale [6-9] and even less investigate the applicability of flax fibre-reinforced laminates in aerospace [10, 11]. In fact, plant fibre composites are good candidates to be used for lightweight structural applications due to their high specific properties, however, there are still many technological and scientific barriers to break down to obtain fully optimised biocomposites for structural applications and high-added value products. It is mainly concerned with improving material durability, refining predictive models and developing robust design methods.

Several European projects (BRIGHT, NATEX, TEXFLAX, BIOBUILD, SSUCHY) have worked to manufacture aligned and continuous reinforcements from discontinuous technical plant fibres, particularly flax fibres [12]. Textile methods, involving fibre spinning and weaving of spun yarns have been shown to have several detrimental effects on composite properties. In addition to the high cost of these operations, it leads particularly to fibre misalignment and hinders resin impregnation, as well as requiring high energy consumption. To overcome these difficulties, some processes have been developed to produce tapes with perfectly aligned flax fibres [13] or fabrics made from low-twisted hemp rovings [14-15]. Currently, the only mature and commercialised unidirectional plant fibre continuous reinforcement is based on flax fibres and produced by the company Lineo-Ecotechnilin (FlaxTape™).

This work proposes an investigation into the mechanical performance of a flax/epoxy composite that meets the requirements of AC 25-853a standard [16] in terms of self-extinguishing. In addition to these fire-retardant properties and weight constraint, the main requirements to fulfil the specifications and certification rules for semi-structural parts in interiors of aircrafts are mechanical properties (static, fatigue and impact), vibroacoustic properties and environmental compliance (humidity, gas/vapour emission), i.e. all solicitations that play a critical role in the service life of the composite. This paper focuses on the mechanical behaviour, including static, fatigue and impact characterization of autoclave prepreg flax composites considering two stacking sequences: unidirectional $[0]_{12}$ and crossply $[(0/90)_3/\bar{0}]_S$.

2. Materials and Methods

2.1 Matrix phase characterisation

A fire-retardant epoxy polymer, prepolymer XB 3515 GB (Huntsman), combined with hardener Aradur 1571 BD and Accelerator 1573 BD is used to impregnate flax fibre reinforced composites. This procedure is performed by Lineo-Ecotechnilin (France), which provides not only the prepreg flaxtape, but also the epoxy polymer used during the impregnation process.

The characterization of the polymer matrix follows a procedure during which the polymer is cured in an oven at two dwell temperatures: 120ºC for 1 hr and 140ºC for 4 hrs at the heating rate of 5ºC/min. The bulk density and the apparent porosity are measured by using the Archimedes principle, according to [4]. For this particular test the mass of the sample is considered under three conditions: m_1 (dry mass), m_2 (mass impregnated with water) and m_3 (mass impregnated with water suspended). The dry mass m_1 is obtained by drying the sample at 100± 5ºC until reaching a constant mass. The impregnated mass m_2 is obtained after the samples are placed in vacuum with distilled water for 24 hrs. The mass m_3 is obtained by weighing the saturated sample suspended in water using a basket immersed in the liquid. The bulk density is calculated as the quotient of the dry mass divided by the external volume (m_2 - m_3), including the pores. The apparent porosity is obtained by dividing the volume of the open pores (m_2 - m_1) by the external volume (m_2 - m_3) expressed as a percentage.

An ultra-micro dynamic hardness tester (DUH-211S, Shimadzu) is used to measure the Vickers Hardness (HV) and the elastic modulus (E_{HV}) of the epoxy polymer. Five measurements are taken at 800mN and 1 mN/sec from the same sample test. The shear modulus (G*) is estimated by assuming the matrix behaving as an isotropic material ($G=E/2(1+\nu)$). The Poisson´s ratio (0.35) is obtained from similar epoxy systems [5].

A thermogravimetric analysis has also been performed on the oven-cured epoxy polymer and the flax composite. A Netzsch STA 449 F3 Jupiter analyser using inert atmosphere is here used.

2.2 Flax composite: prepreg and manufacturing

The prepreg has a nominal 50% flax weight fraction. Based however on the density of the matrix and the geometric and weight parameters of the flaxtape, the matrix/fibre volume fractions are estimated at 43/56%. The average diameter of the flax fibres (14.8 µm) has been measured from pictures obtained from backscatter SEM at 5 kV (Hitachi TM-3000), as shown in Figure 1.

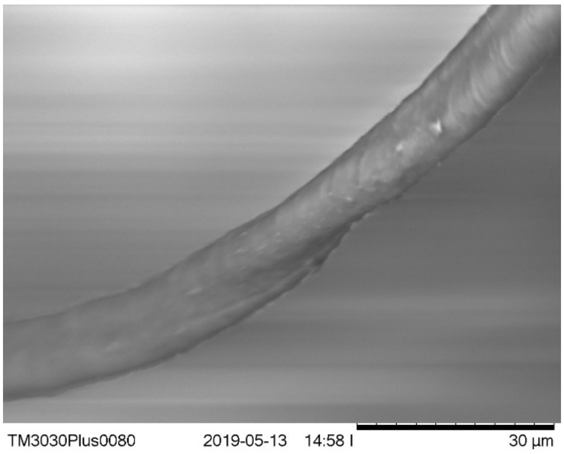

Figure 1. BSE image of single flax fibre.

Twelve (12) and thirteen (13) prepreg flax plies are laid up forming unidirectional $[0]_{12}$ and crossply $[(0/90)_3/\bar{0}]_S$ fibre architectures. The lay-ups are cured at 140°C at 100 psi, according to the autoclave conditions (Figure 2a). An aluminium plate is used on the top surface of the lay-up to obtain a similar finish of the bottom surface and laminates with acceptable flatness. A preliminary study revealed that laminates cured in the same condition without the aluminium plate had rougher surfaces and slight warping due to residual stresses (Figure 2a right side). The UD and cross-ply composites have average thicknesses of 2.05 mm and 2.22 mm respectively, corresponding to approximately 0.17 mm per layer. The samples are machined by Trotec (SP 500) laser cutting machine operating at Power 80, Speed 0.80 and PPI 100 Hz to avoid the swelling effect of traditional liquid-cooled cutting.

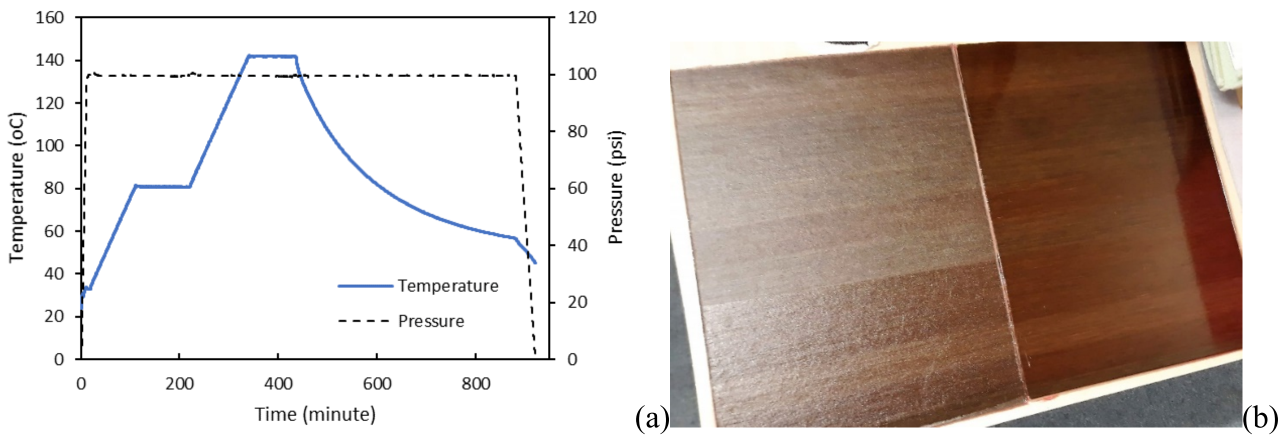

Figure 2. Autoclave manufacturing temperature and pressure profiles (a) and flax composites made without (left image) and with (right image) aluminium plate.

2.3 Flax composites: characterisation

The flax UD and cross-ply composites are evaluated in the longitudinal and transverse directions. Seven (7) UD plies are subjected to longitudinal loads and six (6) UDs have been loaded in the transverse direction. Absolute and specific properties have been calculated.

2.3.1 Physical properties

The apparent porosity, water absorption, apparent density and bulk density of the flax composites are measured by the Archimedes principle, based on the recommendations of ASTM C1039 [17], as detailed in section 2.1.

The fibre, void and matrix volume fractions are also evaluated by observing pictures of transverse cross-sections from Scanning Electron Microscopy (TESCAN Mira3) operating at 20 kV. Figure 3 shows an example of an image used to recognise and determine the surface area of each constituent. The software and pattern recognition algorithms provided by Tescan were used for the image analysis. The red, yellow and green colour represent respectively the fibre, matrix and void volume fraction.

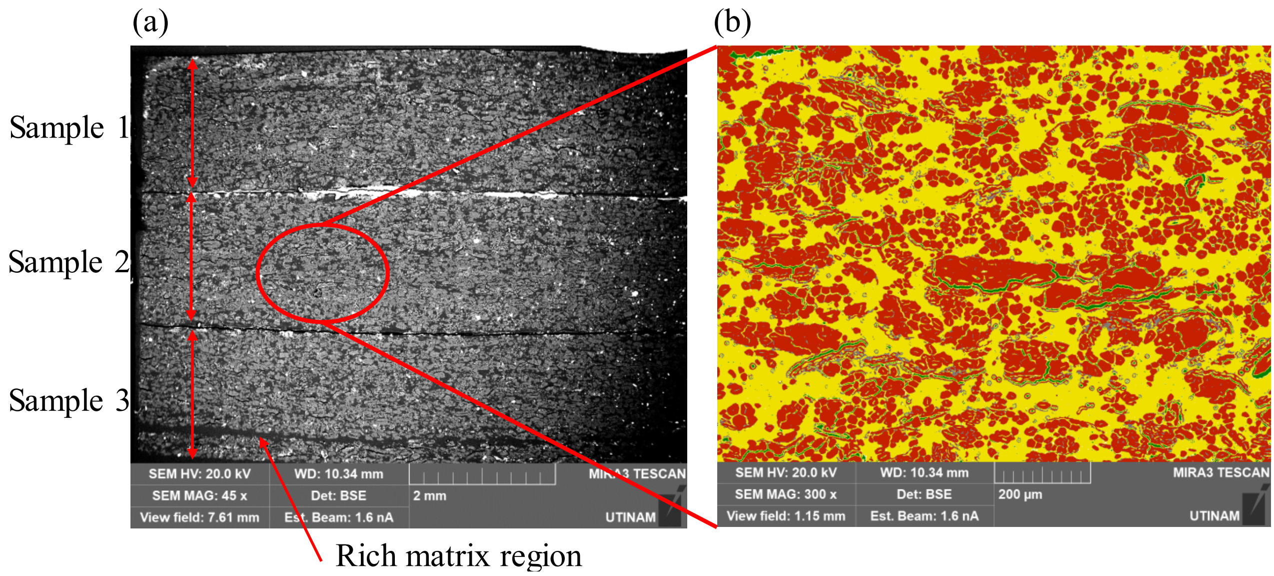

Figure 3. SEM image of 3 unidirectional $[0]_{12}$ specimens in the cross-section (a) and processed image of a specific area (red = fibres, yellow = matrix, and green = porosity) (b).

2.3.2 Tensile properties: longitudinal and transverse fibre directions

Tensile testing is performed along the longitudinal and transverse fibre directions with samples having sizes of $250 \times 15 \times \sim 2$ mm^3 and $170 \times 25 \times \sim 2$ mm^3 respectively, as recommended by the ASTM 3039 [18]. Preliminary tests were performed with and without tab material, and smaller data fluctuations were observed in samples without the tabs. White dots have been applied to the centre and at one quarter of the nominal length (Figure 4a). An Imetrum video-gauge extensometer and an Instron test machine equipped with 100 kN load cell have been used. The crosshead speeds were 2 and 1 mm/min and were applied during the longitudinal and transverse tests, respectively. The modulus of elasticity has been calculated on the stress and strain slopes for strains lower than 0.001 mm/mm.

2.3.3 Bending properties: longitudinal and transverse fibre directions

Three-point bending tests have been performed on UD and crossply flax composites. Five samples of $65 \times 13 \times \sim 2$ mm^3 (Figure 4b) have been here tested (52 mm span fixture and 2 mm/min test speed according to ASTM D790 [19]). An Instron testing machine equipped with 1 kN load cell is used.

2.3.4 Shear properties

The shear strength and modulus are determined in an indirect way by tensile loading of UD and crossply flax composites with fibres oriented at 45° and ±45°, respectively. Five (5) specimens of size $175 \times 25 \times \sim 2$ mm^3 are tested according to ASTM 3518 [20] (Figure 4c). An Instron 100 kN test machine is used in this case with a speed of 1 mm/min. The Imetrum video-gauge extensometer is also used to measure strains in the transverse and longitudinal directions based on the white dots drawn on the samples (Figure 4c).

2.3.5 Impact properties (Drop Tower): longitudinal and transverse fibre directions

The impact test has been carried out using an Instron Drop weight impact tester (Dynatup 8250). Tests have been performed at 14 J and 1.95 m/s, without rebound impact. The amount of energy has been specified at 6.7 J/mm (energy/sample thickness ratio), as recommended by the ASTM D7136 standard [21]. The data acquired during the test were related to the deflection at maximum load (mm), the maximum load (kN), the impact velocity (m/s), the total energy (J) and the total time (ms) [21]. The samples had sizes of 100×150 mm^2, with the support cut out equal to 75×125 mm^2 (Figure 4c).

2.3.6 Fatigue properties: longitudinal fibre direction

The tensile-tensile fatigue tests are performed using an Instron Eletropuls E10000 machine equipped with a 10 kN load sensor, on the flax composites UD $[0]_{12}$. The axial strain is measured using an MTS 632-31F clip-on extensometer, with a gauge length of 50 mm (measurement range: +8%/-2%), as shown in Figure 4e. The tensile stress is computed by dividing the applied load by the initial cross-section of the specimen. The fatigue tests are realized under a sinusoidal waveform loading at a loading frequency of 30 Hz, using a load amplitude control mode. Results from a previous study [22], showed that 30 Hz is a suitable frequency for the characterization of the fatigue behaviour of such composite materials. The ratio between minimum and maximum stress (R) is 0.1. Six levels of maximum stress are applied, i.e. 75, 67, 58, 50, 45 and 40% of the mean quasi-static strength. At least 3 specimens are tested at each level. The tests are conducted until the failure of the specimens. The dimension of specimen is $200 \times 15 \times 2$mm^3. Specimens are tested without tab materials. The average and peak-to-peak load and strain amplitudes are measured and recorded for each cycle. A complete cycle is also recorded as a function of a linear progression whose common difference depends on the stress level and thus fatigue test duration. The last 20 cycles before breaking are also systematically recorded. The apparent modulus is determined using linear regression of stress/strain curve between 0.01% and 0.15% of strain.

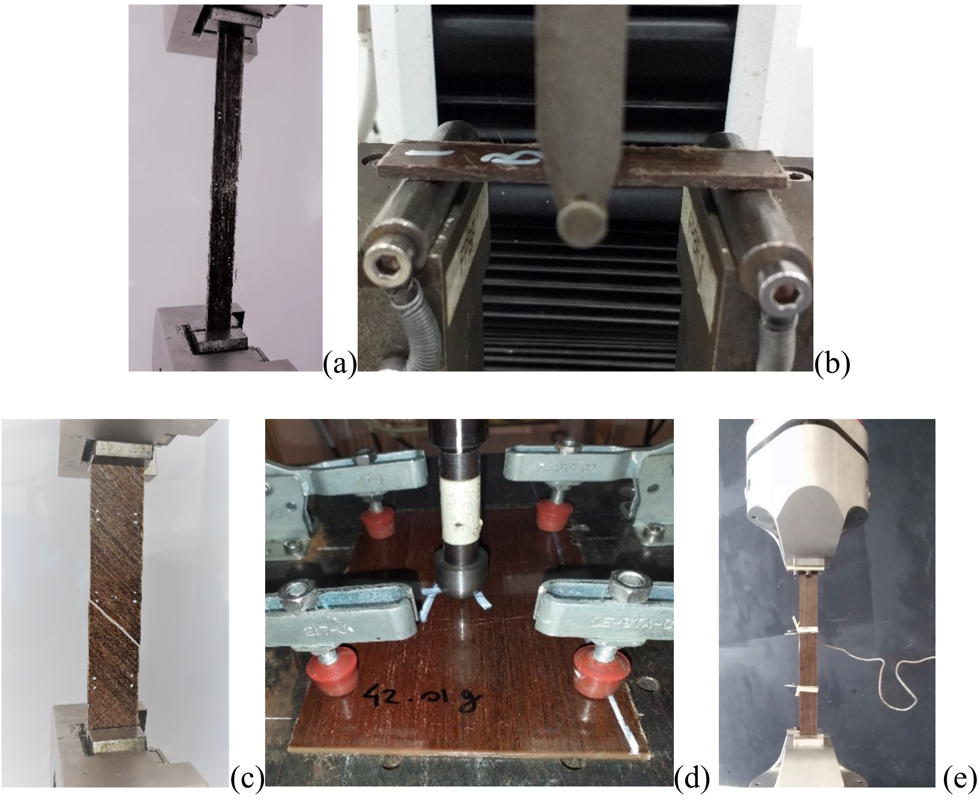

Figure 4. Tensile (a), bending (b), shear (c), impact (d) and tensile-tensile fatigue (e) test configurations.

2.3.7 Comparison study: UD glass and flax fibre composites

In order to better assess the structural performance of flax composites as a potential substitute for glass fibre composites in secondary structural applications, a comparison is made based on their specific properties. The properties of unidirectional E-glass fibre composites, including bulk density of 1.85 g/cm^3, are obtained from the Matweb® data sheet [23].

3. Results

3.1 Matrix phase

Table 1 shows the bulk and apparent densities, apparent porosity and water absorption averages and standard deviations (SD) for the epoxy polymer. The increased porosity (4.91%) and the water absorption (4.24%) can be attributed to the presence of macro pores in the samples due to the curing process in the vacuum-free oven. The measured bulk density of 1.16 is in accordance with Huntsman datasheet.

Table 1. Properties obtained via Archimedes principle.

Property	Average	SD
Apparent porosity (%)	4.91	0.01
Water absorption (%)	4.24	0.01
Apparent density (g/cm^3)	1.22	0.01
Bulk density (g/cm^3)	1.16	0.01

Table 2 shows the Hardness Vickers, the elastic modulus and the predicted shear modulus for the fire-retardant epoxy polymer. The modulus of elasticity is slightly higher than the range of 2.9 to 3.10 MPa provided by Huntsman datasheet for the flexural modulus.

Table 2. Elastic modulus and Hardness Vickers of the epoxy matrix.

Property	Average	SD
Modulus of elasticity (GPa)	3.39	0.08
Hardness Vickers (HV)	24.38	0.54
Shear modulus (GPa)	1.26	0.03

Figure 5 shows the results of the thermogravimetric analysis performed on the epoxy polymer and the flax composite. The DrTGA curves indicate different ranges of thermal degradation for both the composite and the epoxy resin. The DrTGA curve of the composite shows mass loss from 20°C (room temperature) to 150°C (point a). The thermal events also present in the curve are related to the removal of the residual moisture from the composite. The event marked at point b indicates the thermal degradation of the hemicellulose from the flax fibres. Hemicellulose in general degrades before cellulose, with degradation occurring between 320°C and 350°C [24]. In our case, the cellulose degradation is present at point c. Degradation of the epoxy resin contained in the composite is also present (point d). Note that the epoxy resin presents a single degradation process between 340°C and 420°C, with a 51% mass loss with a peak at 406°C (point e). The absence of mass loss and/or thermal events at temperatures below 100°C indicates the absence of residual moisture absorbed by the environment.

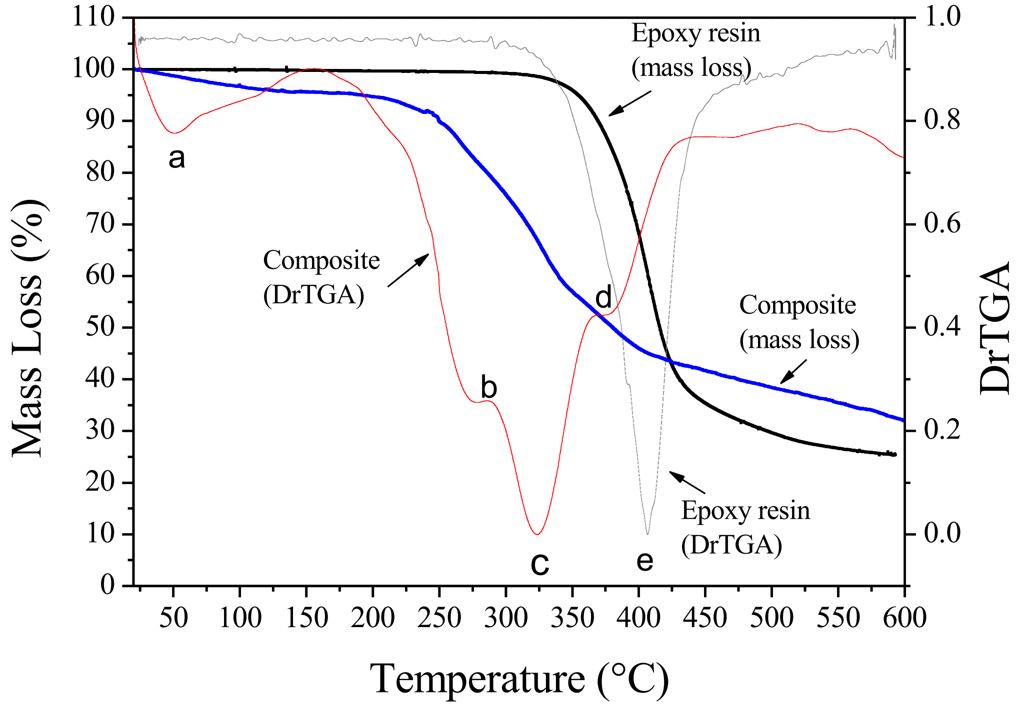

Figure 5. Thermogravimetric analysis of the epoxy polymer and flax composite.

3.2 Flax composite

3.2.1 Physical properties

Table 3 shows the physical properties of the flax composites obtained via Archimedes and Image analysis. There was no significant difference in physical properties between UD and crossply composites. A 7.37% apparent porosity level is obtained, which may affect the durability of natural fibre composites, especially under high humidity environments. Phillips *et al.* [25] investigated the porosity level of autoclaved flax/epoxy prepreg composites via image analysis, revealing a large variation from 1% to 20%. The porosity level (~8.88%) measured by image analysis is nearly 20% higher than those obtained via water immersion. The fibre/matrix volume fraction is 52/39%, slightly lower than the 56/43% estimate as the latter does not consider void volume.

Table 3. Physical properties of flax composites.

Method	Property	Average	SD
Archimedes	Apparent porosity (%)	7.37	1.03
	Water absorption (%)	5.44	0.76
	Apparent density (g/cm^3)	1.38	0.01
	Bulk density (g/cm^3)	1.26	0.01
Image analy	Porosity (%)	8.8	1.3
	Fibre (%)	52.6	3.1

	Matrix (%)	38.8	4.7

3.2.2 Tensile properties: UD and crossply composites

Table 4 shows the average absolute and specific tensile properties of the UD and crossply flax composites related to the longitudinal and transverse directions. The Poisson´s ratio (0.38±0.02) is measured for the UD composites loaded along the longitudinal direction. Crossply composites are made here from 13 plies; the tensile tests along the longitudinal and transverse directions are however performed with samples with 7 and 6 plies aligned to the load direction, respectively. A typical stress and strain curve is plotted for each type of composite tested (Figure 6). Significant increases in stiffness (8 times), strength (16 times) and elongation (4 times) are obtained from UD composites tested along the longitudinal and transverse directions, respectively (Figure 6a). Crossply composites loaded along the longitudinal direction show a slight improvement in terms of mechanical performance compared to the ones subjected to transverse load, since they have 7 load-oriented plies instead of 6 (Figure 6b).

As shown in Figure 6a, higher tensile strength, modulus and strain at failure levels are present in the UD flax composites tested along the longitudinal load direction due to their 12 plies under tension (Table 4). A drastic 8-fold reduction in tensile modulus is observed for UD composites tested in the transverse direction. In addition, a 75% reduction in stiffness is observed when crossply composites (7 plies) are tested in the longitudinal direction; this corresponds to 71% of the load-oriented fibres compared to the UD composites case (12 plies). The tensile strength of crossply composites is also decreased by 88% compared to the one provided by the UD composites. Crossply composites give however increased specific properties in the transverse direction. In general, UD and crossply composites tested along the two directions exhibit a brittle fracture mode, with cracks transversely oriented along the sample cross section (Figure 7). Srb *et al.* [26] have tested autoclaved UD flax composites under the longitudinal and transverse fibre directions. Their tensile stiffness and strengths were of 9.05GPa and 159.83 MPa respectively in the longitudinal loading case, and 1.25 GPa and 6.61 MPa in the transverse one. These values are lower than the ones obtained in the present work (Table 4). Phillips *et al.* [25] obtained the elastic modulus (11GPa), tensile strength (94 MPa) and strain (0.0139 mm/mm) for autoclaved flax/epoxy composites made of three layers of crossply flax fabric and 45% fibre volume fraction. Not only a reduced fibre volume fraction, but also the fabrics obtained by fibre spinning are primarily responsible for reduced properties. Berges *et al.* [27] also investigated autoclaved UD flax/epoxy composites composed of 50% fibre volume fraction. Similar mechanical properties were obtained along longitudinal and transverse load directions.

Table 4. UD and crossply composites: tensile properties.

Load direction	Type	E_T (GPa)	E_T/ρ (GPa/g.cm^{-3})	σ_T (MPa)	σ_T/ρ (MPa/g.cm^{-3})	Strain (mm/mm)	Plies under tension
Longitudinal	$[0]_{12}$	35.6 ±4.7	28.3	300.5± 22.5	238.5	0.018 ± 0.002	12 plies
	$[(0/90)_3/\bar{0}]_S$	20.3±2.1	14.7	158.4±16.4	16.4	0.010 ± 0.004	7 plies
Transverse	$[0]_{12}$	4.35±0.4	3.4	19±1.7	15.1	0.005 ± 0.001	zero
	$[(0/90)_3/\bar{0}]_S$	19.9±2.5	15.9	146.9±16.7	117.5	0.010 ± 0.001	6 plies

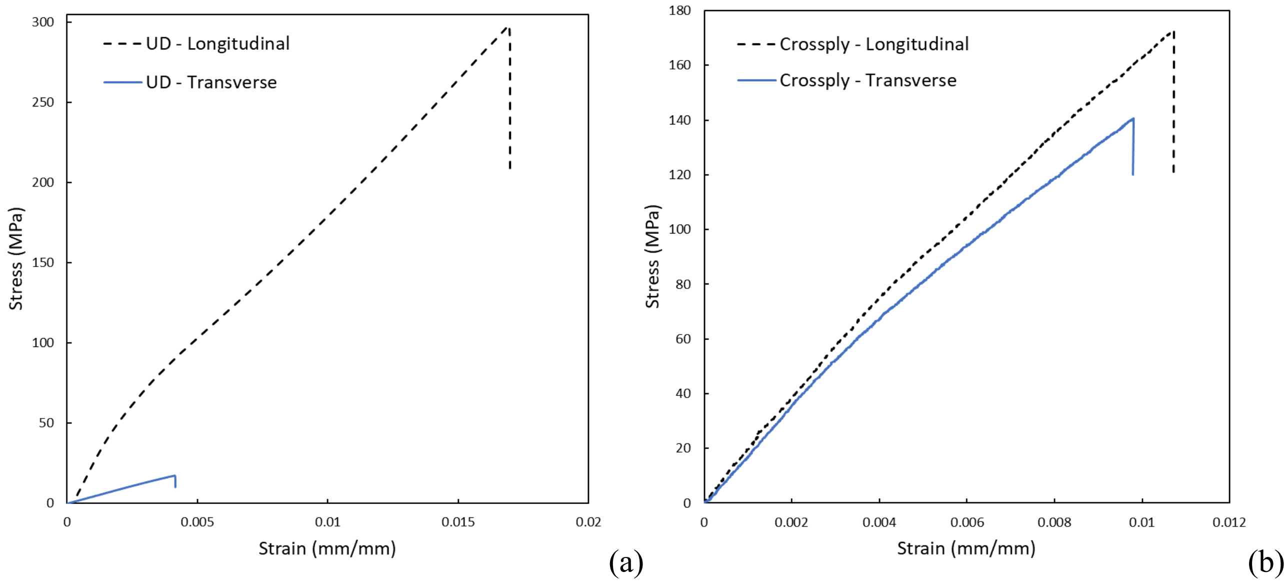

Figure 6. Typical tensile behaviour of UD (a) and Crossply (b) flax composites.

Figure 7. Tensile fractures of samples tested in longitudinal (a) and transverse (b) directions.

3.2.3 Fatigue behaviour of UD composites

The S-N curve obtained for the UD composite is presented in Figure 8. Results show a gradual decline in fatigue strength with increasing number of fatigue cycles. The order of magnitude is in agreement with previous results collected in a similar non-fire-retardant flax-preg composites [22], and more generally for flax/epoxy laminates [28-30]. Among plant fibres, flax has shown to impart high fatigue resistance to composites, higher than hemp and comparable to the one provided by sisal and jute [31]. Even if for some levels of maximum strength (135 and 175 MPa for example) the dispersion is relatively important, the fatigue strength as a function of number of cycles is however appropriately fitted by a power-law curve. Interestingly, the maximum stress for 1 M cycles is approximately 150 MPa, representing roughly 50% of the quasi-static strength. As it was already demonstrated [22], for this type of material, the maximum stress continues to decrease as a function of increasing number of cycles. For 10^8 cycles, the maximum stress is thus approximately 125 MPa, a value that remains however very attractive for engineering applications.

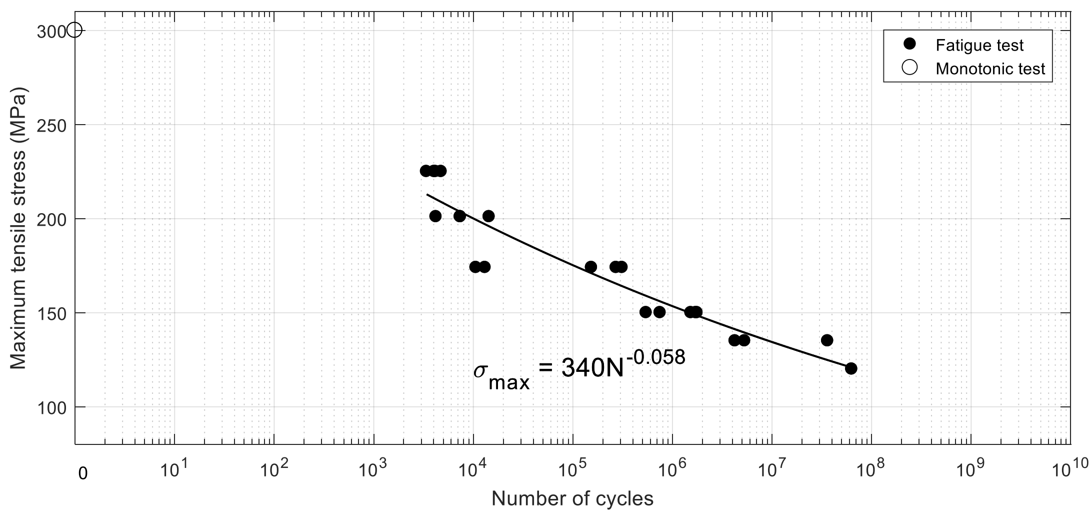

Figure 8. S-N curves for tensile-tensile fatigue of UD composite.

Open literature often refers to a stiffening effect provided by flax/epoxy composite materials during fatigue tests [22, 27-33], at least when those tests are carried out under tension and load-control conditions. The origin of this unusual behaviour in laminates is not fully understood and is currently highly debated in the literature [32]. For the present study, an increase in the apparent modulus with the increasing number of cycles is only observed for the lowest loading levels. The increase reaches up to 8% for the lower loading levels (Figure 9a). First, the apparent stiffness significantly increases until a life fraction of 0.05 and then stabilised during most of the fatigue life. A slight decrease is then observed just before the specimen failure. For the highest loading levels the stiffening effect is certainly counterbalanced by the damage progression in the composite which results in a progressive decrease of the apparent stiffness in the second stage. The mean strain increases with the increasing number of cycles (Figure 9b), reflecting the time-dependent behaviour of this type of composites and the fatigue-creep coupling in the fibre direction in tension-tension fatigue tests.

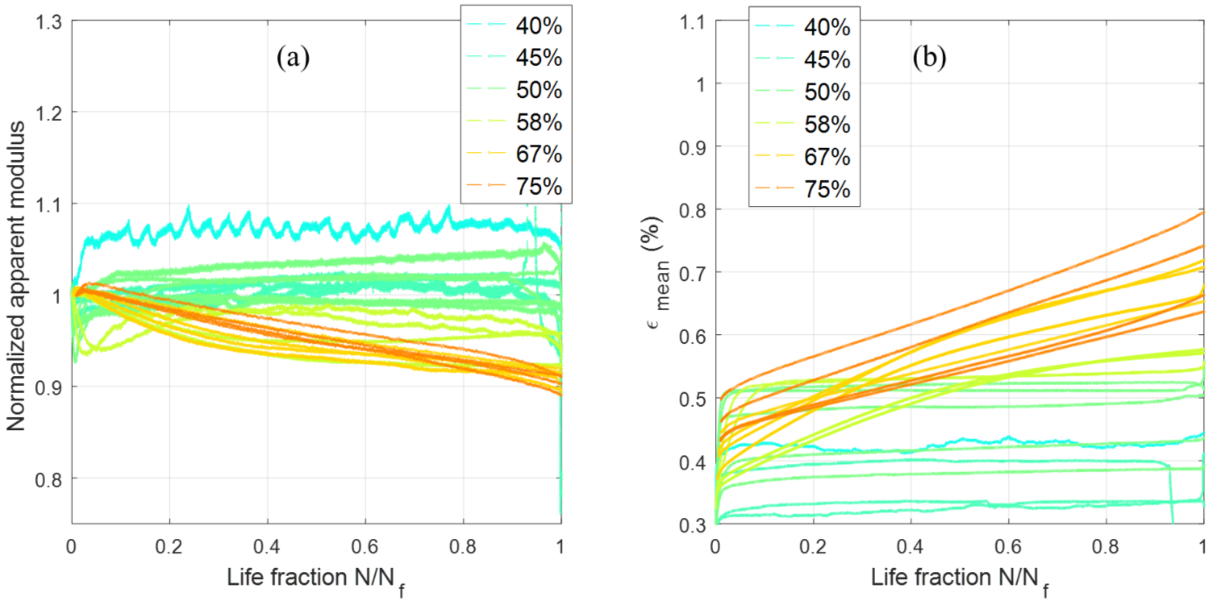

Figure 9. Normalized apparent modulus and mean strain during the fatigue tests.

3.2.4 Bending properties: UD and crossply composites

Figure 10 shows the mechanical behaviour of the composites under three-point bending test. A transverse crack is observed for both UD and crossply configurations (Figure 11). Table 5 shows the absolute and specific bending properties, as well as the number of plies aligned with the tensile loads located below the neutral line. The compressive loads located on the upper beam side are largely dominated by the properties of the matrix [34]. On the other hand, the presence of fibres aligned with the tensile loads on the lower beam side plays an important role in the bending behaviour of the laminates. An 8-fold reduction in flexural modulus is observed between the UD flax composites in the 0° and 90° configurations. The latter are dominated by the properties of the matrix (E ~3.4GPa, see Table 2), since no ply is oriented along the load direction. A 50% decrease in flexural stiffness is also obtained for crossply composites tested along the longitudinal direction relative to the UD configuration. This behaviour is also related to the 50% reduction in the number of plies under tension (Table 5). It is noteworthy that the crossply composites tested longitudinally are 120% stiffer than those tested along the transverse direction. Although they possess the same number of plies aligned to the tensile loads (3), the first 0° oriented ply is located at the bottom surface, while the first ply subjected to tension is at 90° and it is the second in the stacking sequence. This affects the global distribution of axial stresses. In addition, other plies under tension are closer to the neutral line, therefore reducing their stiffening effect on the overall bending modulus. A similar behaviour has been discussed by Junior *et al.* [34] in a glass fibre composite with unbalanced beam stiffness due to the inclusion of rigid particles in the matrix phase. It is also worth of notice that the seventh ply located on the neutral line does not contribute to axial stresses through bending loads.

The flexural strength follows a similar behaviour to the flexural stiffness one (Table 5). Higher displacements (Figure 8) and strains at failure (Table 5) are present in composites tested along the longitudinal direction. Crossply composites transversely tested show however a similar strain to failure level compared to those tested along the longitudinal direction. Cross-ply composites also show two levels of failure strains when compared to transversally tested UD composites. This behaviour also reveals that crossply flax composites are preferable for structural applications, as they combine strength and stiffness in both directions of the load. The specific properties follow the same trend as the absolute ones, since no significant change in density is present.

Some autoclaved UD flax composites have been subjected to three-point bending along the longitudinal and transverse fibre directions [25]. The flexural stiffness (strength) of 2.31 GPa (29.95 MPa) and 0.67 GPa (16.87 MPa) along the longitudinal and transverse direction reported in that reference are lower than the properties measured in the present work (see Table 5).

Table 5. UD and crossply composites: 3PB properties.

Load direction	Type	E_B (GPa)	E_B/ρ (GPa/g.cm^{-3})	σ_B (MPa)	σ_B/ρ (MPa/g.cm^{-3})	Strain at failure (mm/mm)	Plies under tension
Longitudinal	$[0]_{12}$	24.56 ± 3.77	19.5	332.09 ± 7.38	263.6	0.015 ± 0.001	6 plies
	$[(0/90)_3/\bar{0}]_S$	12.74 ± 1.38	9.7	185.91 ± 7.87	141.9	0.020 ± 0.001	3 plies
Transverse	$[0]_{12}$	3.28 ± 0.37	2.6	29.87 ± 2.59	11.5	0.010 ± 0.001	zero
	$[(0/90)_3/\bar{0}]_S$	5.75 ± 0.88	4.2	103.83 ± 2.95	81.09	0.021 ± 0.002	3 plies

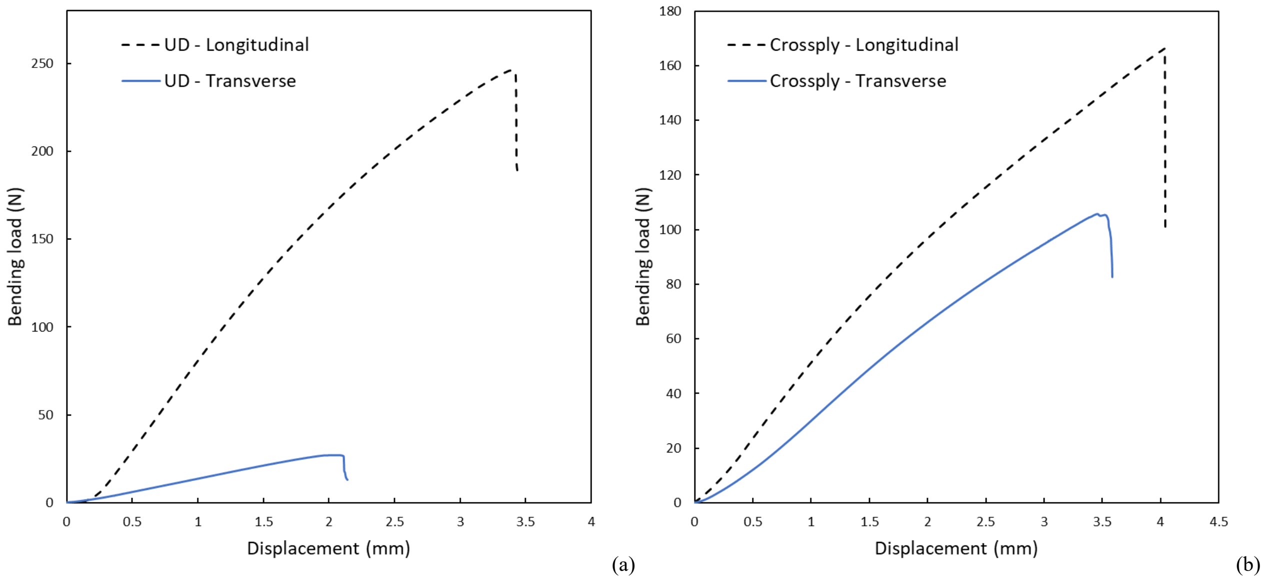

Figure 8. Typical bending behaviour of UD (a) and crossply (b) flax composites.

Figure 9. Bending fractures of samples tested in longitudinal (a) and transverse (b) directions.

3.2.5 Shear properties

Table 6 shows the shear properties of the UD and crossply composites. Although the shear modulus is quite similar, a significant increase in shear strength (also specific) is observed in crossply laminates; this is because of the presence of ±45° oriented fibres, while the UD architectures possess only fibres at +45°. The shear deformation at failure is also four times larger in crossply composites with a consequent increase in toughness (Figure 10). The fracture of the UD composites is characterised by a 45° crack along the flax fibre orientation (Figure 11a), while the crossply composites show a transverse crack along the central part of the sample (Figure 11b) due to the ±45° oriented fibres.

Table 6. UD and crossply composites: shear properties.

Composite type	G (GPa)	Specific (GPa/g.cm^{-3})	τ (MPa)	Specific (MPa/g.cm^{-3})	Shear deformation at failure (mm/mm)
UD (+45°)	4.29 ± 0.59	3.4	37.74 ± 2.92	29.9	0.009 ± 0.001
Crossply (±45°)	4.20 ± 0.23	3.1	84.95 ± 3.88	62.92	0.039 ± 0.004

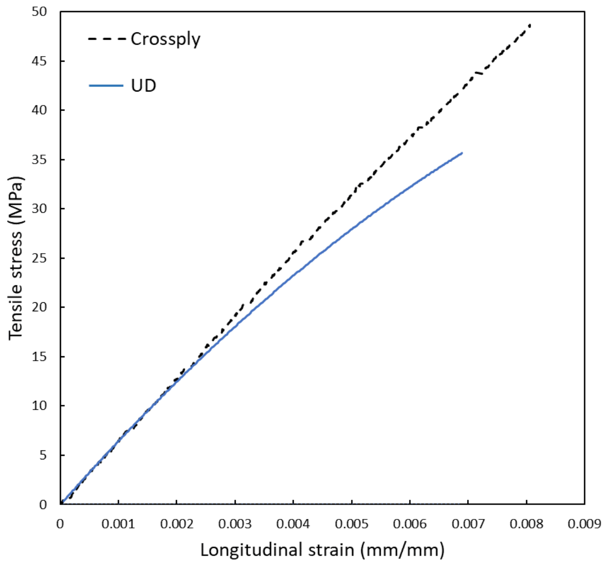

Figure 10. Mechanical behaviour of UD and crossply flax composites under shear load via tensile testing.

Figure 11. Shear fractures of UD (a) and crossply (b) samples.

3.2.6 Impact properties (Drop Tower)

Table 7 shows the impact properties in bending mode of the UD flax composites tested in the longitudinal and transverse directions. The longitudinal and transverse directions correspond to UD fibres oriented along the "length" and "width" support, respectively. The stiffer bending crossply composite measured along the longitudinal direction (see Table 5) shows an increased impact energy (6.12 J) and deflection at maximum load (9.09 mm). In general, a more rigid static mechanical structure provides a reduced Charpy impact energy [35]. It is noteworthy that the samples here are simply supported across the edges. In this case, the fibres oriented along the transverse direction contribute substantially to increase the stiffness of the composite with overall lower values of deflection (8.09 mm) and total absorbed energy (4.91 J).

Table 7. Impact properties: longitudinal versus transverse directions.

Load direction	Deflection at max load (mm)	Maximum load (kN)	Impact velocity (m/s)	Total energy (J)	Total time (ms)
Longitudinal	9.09 ± 0.99	0.50 ± 0.02	1.95 ± 0.01	6.12 ± 0.24	12.52 ± 0.05
Transverse	8.04 ± 0.49	0.49 ± 0.03	1.96 ± 0.01	4.91 ± 0.91	7.70 ± 1.03

Figure 12 shows the impact behaviour of typical samples tested in the longitudinal and transverse fibre directions. Two red lines are drawn on the impact load versus deflection slope to show that the transverse samples behave stiffer than the longitudinal crossply composites, which demonstrates the reinforcing effect provided by the transverse fibres oriented along the width of the support. Two green dashed vertical lines are also plotted to show the region (from ~8 to ~9 mm) of the maximum impact loads. The two green lines indicate when the composite fails (drop-in load). Note that the longitudinal UD composites provide a greater impact energy up to a deflection of 15 mm. After this point, the transverse samples show an increased impact absorption due to the additional energy to break the transverse flax fibres (Figure 13a). In contrast, the crack propagation of the longitudinal samples occurs along the matrix-fibre interface (Figure 13b), leading to a lower impact energy absorption after fracture (Figure 12).

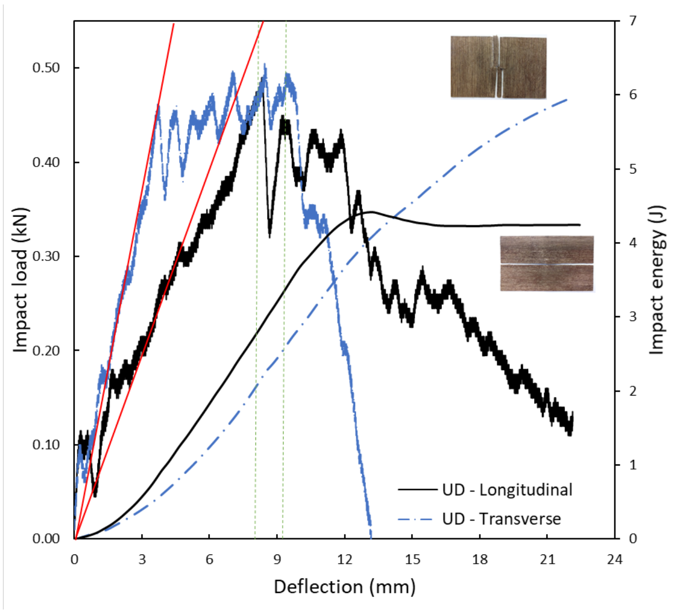

Figure 12. Impact responses for typical UD samples tested in the longitudinal and transverse fibre directions.

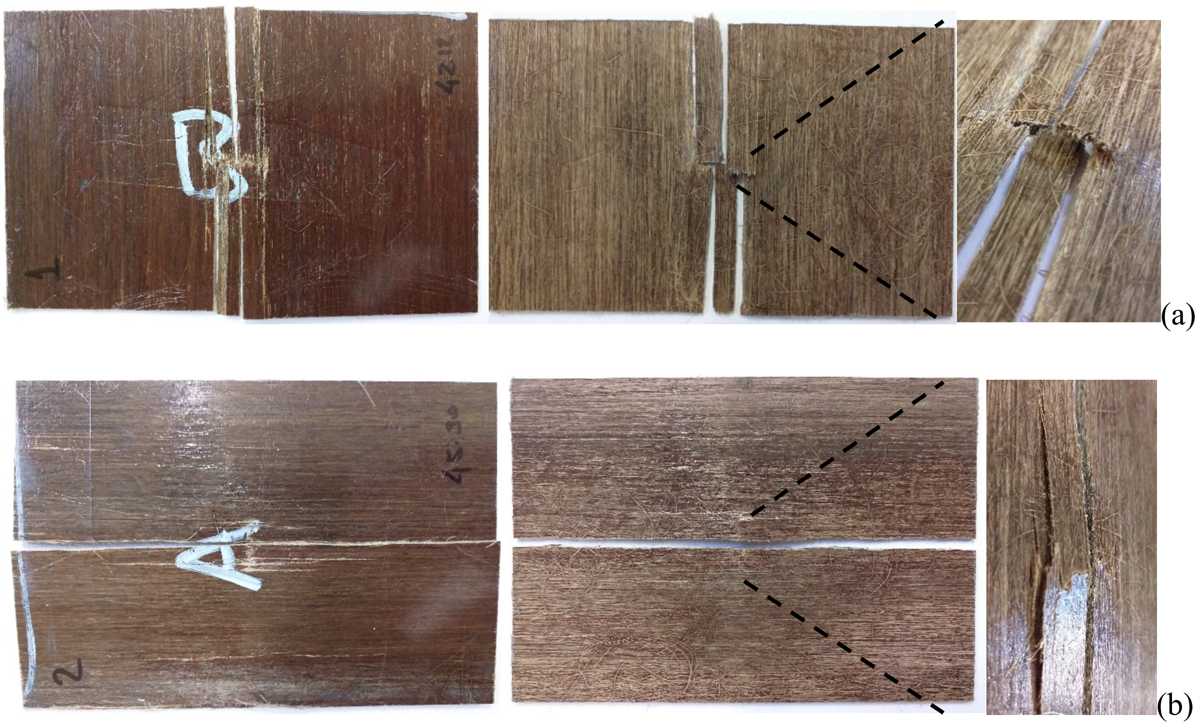

Figure 13. Impact specimens after testing: (a) transverse and (b) longitudinal fibre directions.

3.2.7 Flax and glass fibre composites: a comparison

Table 8 shows the specific properties for tensile, flexural and shear loadings considering the bulk densities of 1.26 g/cm^3 and 1.38 g/cm^3 for UD flax and glass fibre composites, respectively. The highest values are highlighted in bold and percentage variations are calculated to compare the results. Flax composites are not superior to glass fibres under bending loads; however, their specific tensile modulus along the longitudinal direction is larger, which makes flax composites a favourable condition for the replacement of glass fibre composites in structural applications. In addition, the specific shear strength of flax composites is 129% higher than glass composites. On the other hand, the specific shear modulus of glass fibre composites is 12 times higher than flax composites. The transverse tensile properties are basically dependent on the characteristics of the matrix phase.

Shah *et al.* [8] concluded that flax composites are a suitable structural replacement for E-glass in small wind turbine blade applications. The flax/polyester composite blade, manufactured by resin transfer mould, is 10% lighter than E-glass/polyester and meets structural integrity requirements under "normal" and "worst" operating conditions. In contrast, Blanchard and Sobey [5] performed a comparative design of E-glass and flax structures based on reliability, concluding that the flax structure needs to be 2.4 times heavier than E-glass structures for equivalent safety. It is noteworthy that the mechanical properties of flax composites taken from the literature [5] are substantially lower to those obtained in the present work, especially the longitudinal elastic modulus (6.62 MPa) and strength (6.86 MPa) and shear strength (5.04 MPa). This may justify the pessimistic consideration made by the authors [5] about flax composites.

Table 8. Specific properties of glass and flax fibre composites.

<table>
<tr><th>Load direction</th><th>Specific properties (MPa/g.cm^{-3})</th><th>Glass fibre composite</th><th>Flax fibre composite</th><th>Percent variation (%)</th></tr>
<tr><td rowspan="4">Longitudinal</td><td>Tensile strength</td><td>521.6</td><td>238.5</td><td>↓118%</td></tr>
<tr><td>Tensile modulus</td><td>21.2</td><td>28.3</td><td>↑33%</td></tr>
<tr><td>Flexural strength</td><td>621.6</td><td>263.6</td><td>↓136%</td></tr>
<tr><td>Flexural modulus</td><td>20.9</td><td>19.5</td><td>↓7%</td></tr>
<tr><td rowspan="4">Transverse</td><td>Tensile strength</td><td>10.8</td><td>15.1</td><td>↑39%</td></tr>
<tr><td>Tensile modulus</td><td>5.2</td><td>3.4</td><td>↓118%</td></tr>
<tr><td>Flexural strength</td><td>40.9</td><td>11.5</td><td>↓255%</td></tr>
<tr><td>Flexural modulus</td><td>5.9</td><td>2.6</td><td>↓129%</td></tr>
<tr><td rowspan="2">45°</td><td>Shear strength</td><td>13.0</td><td>29.9</td><td>↑39%</td></tr>
<tr><td>Shear modulus</td><td>40.9</td><td>3.4</td><td>↓1100%</td></tr>
</table>

Finally, the higher specific tensile modulus and similar specific flexural modulus of UD flax composites relative to E-glass composites makes them an attractive material for secondary structural applications. The authors emphasise that the use of flax composites as a sandwich panel skins is quite promising, as shown by CoDyre *et al.* [36]. A three-layered flax composite skin, only 17% thicker than a single-layer E-glass skin, led to equivalent flexural and axial strengths in sandwich panels made of PIR foam cores.

4. Conclusions

In this paper autoclaved flax composites made with unidirectional and crossply fibres have been characterised and benchmarked. The main conclusions that can be drawn from this work are the following:

i. The fire-retardant epoxy polymer used in the prepreg possesses elastic and shear moduli of 3.39 GPa and 1.26 GPa, respectively.

ii. The TGA analysis indicates a thermal stability of up to 300^{o}C, with subsequent significant drop in mass loss from 340^{o}C and 420^{o}C.

iii. The flax composites exhibit a porosity of 7.4%, a water absorption of 5.4% and an apparent density of 1.38 g/cm^3.

iv. The UD composites tested along the 0^{o} direction show an 8-fold increase in stiffness compared to the laminates loaded along the transverse direction. The same happens for the strength and elongation at failure (16-fold and 4-fold, respectively). Tensile strength and stiffness of the crossply composites are reduced by almost 80% compared to the UD configuration. The UD flax composites have a Poisson´s ratio of 0.38 under tensile loading (0^{o}).

v. An 8-fold reduction of the flexural modulus is observed between the UD flax composites tested in the longitudinal and transverse directions. A 50% reduction in flexural stiffness is also obtained for crossply composites tested in the longitudinal direction relative to the UD configuration. Longitudinally tested crossply composites are 120% stiffer than those tested along the transverse direction. The flexural strength reveals a similar behaviour to the flexural stiffness one.

vi. Similar shear modulus are obtained for the UD and crossply architectures. The latter however exhibit a 125% increase of shear strength due to the presence of the ±45^{o} oriented fibres.

vii. The UD composites tested longitudinally under bending impact absorb a larger amount of energy and show a higher deflection at maximum load compared to the composites with the 90^{o} architecture. In contrast, transversely tested UD composites possess an increase of impact energy after frature due to the propagation of cracks across the fibres.

viii. A maximum stress is approximately 150 MPa for 1 M cycles, representing roughly 50% of the quasi-static strength. The maximum stress is nearly 125 MPa after 108 cycles, which is still attractive for engineering applications. The apparent stiffness significantly increases until a life fraction of 0.05 and then stabilised during most of the fatigue life.

ix. Higher specific tensile modulus and similar specific flexural modulus of UD flax composites relative to E-glass composites makes them a promising sustainable material for aircraft, transport and lightweight construction designs.

Future work will focus on understanding their environmental performance, durability and moisture resistance.

Acknowledgement

This project has received funding from the Bio Based Industries Joint Undertaking under the European Union's Horizon 2020 research and innovation programme under grant agreement No 744349 (SSUCHY project). The authors would like to acknowledge Stani Carbillet for the SEM characterization.

References

[1] Allaby R, Peterson G, Merriwether D, Fu Y B. (2005). Evidence of the domestication history of flax (Linum usitatissimum L.) from genetic diversity of the sad2 locus. Theor Appl Genet 2005; 112 (1): 58–65. doi:10.1007/s00122-005-0103-3. PMID 16215731.

[2] Ramesh M. Flax (Linum usitatissimum L.) fibre reinforced polymer composite materials: A review on preparation, properties and prospects. Prog Mater Sci 2019; 102:109-166. https://doi.org/10.1016/j.pmatsci.2018.12.004

[3] Yana L, Chouw N, Jayaraman K. Flax fibre and its composites – A review. Compos Part B-Eng 2014; 56:296-317. https://doi.org/10.1016/j.compositesb.2013.08.014

[4] Bourmaud A, Beaugrand J, Shah D U, Placet V, Baley C. Towards the design of high-performance plant fibre composites. Prog Mater Sci 2018; 97:347-408. https://doi.org/10.1016/j.pmatsci.2018.05.005

[5] Blanchard J M F A, Sobey A J. Comparative design of E-glass and flax structures based on reliability. Compos Struct 2019; 225(1):111037. https://doi.org/10.1016/j.compstruct.2019.111037

[6] Bambach M R. Compression strength of natural fibre composite plates and sections of flax, jute and hemp. Thin Wall Struct 2017; 119:103-113. https://doi.org/10.1016/j.tws.2017.05.034

[7] Blanchard J M F A, Mutlu U, Sobey A J, Blake J I R. Modelling the different mechanical response and increased stresses exhibited by structures made from natural fibre composites. Compos Struct 2019; 215(1):402-410. https://doi.org/10.1016/j.compstruct.2019.02.042

[8] Shah D U, Schubel P J, Clifford M J. Can flax replace E-glass in structural composites? A small wind turbine blade case study. Compos Part B-Eng 2013; 52:172-181. https://doi.org/10.1016/j.compositesb.2013.04.027

[9] Shah D U. Damage in biocomposites: Stiffness evolution of aligned plant fibre composites during monotonic and cyclic fatigue loading. Compos Part A-Appl S 2016; 83:160-168. https://doi.org/10.1016/j.compositesa.2015.09.008

[10] Strohrmann K, Hajek M. An Eco-Efficient Helicopter Tailplane Hybridized from Flax, Balsa and Carbon, In: AIAA Scitech 2019 Forum. San Diego, January, 2019. https://doi.org/10.2514/6.2019-0771

[11] Strohrmann K, Hajek M. Bilinear approach to tensile properties of flax composites in finite element analyses. J Mater Sci 2019; 54:1409-1421. https://doi.org/10.1007/s10853-018-2912-1

[12] EuCIA – European Composites Industry Association, available at https://eucia.eu/about-eucia/european-projects/

[13] Khalfallah M, Abbès B, Abbès F, Guo Y Q, Marcel V, Duval A, Vanfleteren F, Rousseau F. Innovative flax tapes reinforced Acrodur biocomposites: A new alternative for automotive applications. Mater Design 2014; 64:116-126. https://doi.org/10.1016/j.matdes.2014.07.029.

[14] Corbin A C, Soulat D, Ferreira M, Labanieh A R, Gabrion X, Malécot P, Placet V. Towards hemp fabrics for high-performance composites: Influence of weave pattern and features. Compos Part B-Eng 2020; 181(15):107582. https://doi.org/10.1016/j.compositesb.2019.107582.

[15] SSUCHY project, available at https://www.ssuchy.eu/

[16] AC 25.853-1 standard: Flammability requirements for aircraft seat cushions, ANM-110, Federal Aviation Administration (FAA), USA, 1986. Available at https://www.faa.gov/regulations_policies/advisory_circulars/index.cfm/go/document.information/documentID/22673

[17] ASTM C1039-85. Standard Test Methods for Apparent Porosity, Apparent Specific Gravity, and Bulk Density of Graphite Electrodes, ASTM International, West Conshohocken, PA, 2015. www.astm.org DOI: 10.1520/C1039-85R15.

[18] ASTM D3039 / D3039M-17. Standard Test Method for Tensile Properties of Polymer Matrix Composite Materials, ASTM International, West Conshohocken, PA, 2017. www.astm.org DOI: 10.1520/D3039_D3039M-17.

[19] ASTM D790-17. Standard Test Methods for Flexural Properties of Unreinforced and Reinforced Plastics and Electrical Insulating Materials, ASTM International, West Conshohocken, PA, 2017. www.astm.org DOI: 10.1520/D0790-17.

[20] ASTM D3518 / D3518M-18. Standard Test Method for In-Plane Shear Response of Polymer Matrix Composite Materials by Tensile Test of a ±45° Laminate, ASTM International, West Conshohocken, PA, 2018. www.astm.org DOI: 10.1520/D3518_D3518M-18.

[21] ASTM D7136 / D7136M-15. Standard Test Method for Measuring the Damage Resistance of a Fiber-Reinforced Polymer Matrix Composite to a Drop-Weight Impact Event, ASTM International, West Conshohocken, PA, 2015. www.astm.org DOI: 10.1520/D7136_D7136M-15.

[22] Jeannin T, Gabrion X, Emmanuel R, Placet V. About the fatigue endurance of unidirectional flax-epoxy composite laminates. Compos Part B-Eng 2019; 165(15):690-701. https://doi.org/10.1016/j.compositesb.2019.02.009

[23] Cytec (Solvay Group) Cyply® 1002 Epoxy Fiberglass Composite, Unidirectional, Matweb website at http://www.matweb.com/search/DataSheet.aspx?MatGUID=3f2253a553404b13893830617250b5d8&ckckr =1.

[24] Santos J C, Siqueira R L, Vieira L M G, Freire R T S, Mano V, Panzera T H. Effects of sodium carbonate on the performance of epoxy and polyester coir-reinforced composites. Polym Test 2018; 67:533-544. https://doi.org/10.1016/j.polymertesting.2018.03.043

[25] Phillips S, Baets J, Lessard L, Hubert P, Verpoest I. Characterization of flax/epoxy prepregs before and after cure. J Reinf Plast Comp 2013; 32(11) 777–785. DOI: 1 0.1177/0731684412473359

[26] Srb P, Syrovátková M, Kulhavý P, Tomková B. Study of Mechanical Properties and Modeling of Flax Reinforced Composites. Mater Sci Forum 2018; 919:152-159. doi:10.4028/www.scientific.net/MSF.919.152

[27] Berges M, Léger R, Placet V, Person V, Corn S, Gabrion X, Rousseau J, Ramasso E, Ienny P, Fontaine S. Influence of moisture uptake on the static, cyclic and dynamic behaviour of unidirectional flax fibre-reinforced epoxy laminates. Compos Part A-Appl S 2016; 88: 165-177. https://doi.org/10.1016/j.compositesa.2016.05.029

[28] Liang S, Gning PB, Guillaumat L. A comparative study of fatigue behaviour of flax/epoxy and glass/epoxy composites. Compos Sci Technol 2012; 72(5):535-43. https://doi.org/10.1016/j.compscitech.2012.01.011

[29] Liang S, Gning P B, Guillaumat L. Properties evolution of flax/epoxy composites under fatigue loading. Int J Fatigue 2014;63(0):36-45. https://doi.org/10.1016/j.ijfatigue.2014.01.003

[30] Shah D U. Damage in biocomposites: Stiffness evolution of aligned plant fibre composites during monotonic and cyclic fatigue loading. Compos Part A-Appl S 2016; 83(Supplement C):160-8. https://doi.org/10.1016/j.compositesa.2015.09.008

[31] Mahboob Z, Bougherara H. Fatigue of flax-epoxy and other plant fibre composites: Critical review and analysis. Compos Part A-Appl S 2018; 109:440-462. https://doi.org/10.1016/j.compositesa.2018.03.034.

[32] Mahboob Z, Bougherara H. Strain amplitude controlled fatigue of Flax-epoxy laminates.

Compos Part B-Eng 2020; 186:107769. https://doi.org/10.1016/j.compositesb.2020.107769.

[33] Bensadoun F, Verpoest I, Van Vuure A W. Residual properties and damage evolution of flax-epoxy composites subjected to fatigue loading. In: 20th International Conference on Composite Materials. Copenhagen, July, 2015. p. 1-10. Available at https://limo.libis.be/primo-explore/fulldisplay?docid=LIRIAS1674575&context=L&vid=Lirias&search_scope=Lirias&tab=default_tab&lang=en_US&fromSitemap=1

[34] Junior A H R, Gomez J E, Hale D W, Tonatto M L P, Panzera T H, Thomas C, Scarpa F. Evaluation of the stiffening mechanism based on micro-sized particle inclusions in laminated composites. Mater Res 2019; 22(4). http://dx.doi.org/10.1590/1980-5373-mr-2019-0084

[35] Dias T C, Panzera T H, Santos J C, Freire R T S, Thomas C, Scarpa F. Epoxy polymers reinforced with carbon microfibre wastes. Mater Today 2019; 8:847-852. https://doi.org/10.1016/j.matpr.2019.02.027

[36] CoDyre L, Mak K, Fam A. Flexural and axial behaviour of sandwich panels with bio-based flax fibre-reinforced polymer skins and various foam core densities. J Sandw Struct Mater 2018; 20(5):595–616. DOI: 10.1177/1099636216667658